Preclinical Efficacy of LP-184, a Tumor Site Activated Synthetic Lethal Therapeutic, in Glioblastoma

Bachchu Lal[1], Aditya Kulkarni[2], Joseph McDermott[2], Rana Rais[3,4,5], Jesse Alt[5], Ying Wu[5], Hernando Lopez-Bertoni[1,3], Sophie Sall[1], Umesh Kathad[2], Jianli Zhou[2], Barbara S. Slusher[3,4,5,6], Kishor Bhatia[2], and John Laterra[1,3,6]

ABSTRACT

Purpose: Glioblastoma (GBM) is the most common brain malignancy with median survival <2 years. Standard-of-care temozolomide has marginal efficacy in approximately 70% of patients due to *MGMT* expression. LP-184 is an acylfulvene-derived prodrug activated by the oxidoreductase PTGR1 that alkylates at N^3-adenine, not reported to be repaired by MGMT. This article examines LP-184 efficacy against preclinical GBM models and identifies molecular predictors of LP-184 efficacy in clinical GBM.

Experimental Design: LP-184 effects on GBM cell viability and DNA damage were determined using cell lines, primary PDX-derived cells and patient-derived neurospheres. GBM cell sensitivities to LP-184 relative to temozolomide and MGMT expression were examined. Pharmacokinetics and CNS bioavailability were evaluated in mice with GBM xenografts. LP-184 effects on GBM xenograft growth and animal survival were determined. Machine learning, bioinformatic tools, and clinical databases identified molecular predictors of GBM cells and tumors to LP-184 responsiveness.

Results: LP-184 inhibited viability of multiple GBM cell isolates including temozolomide-resistant and MGMT-expressing cells at IC_{50} = approximately 22–310 nmol/L. Pharmacokinetics showed favorable $AUC_{brain/plasma}$ and $AUC_{tumor/plasma}$ ratios of 0.11 (brain C_{max} = 839 nmol/L) and 0.2 (tumor C_{max} = 2,530 nmol/L), respectively. LP-184 induced regression of GBM xenografts and prolonged survival of mice bearing orthotopic xenografts. Bioinformatic analyses identified *PTGR1* elevation in clinical GBM subtypes and associated LP-184 sensitivity with EGFR signaling, low nucleotide excision repair (NER), and low *ERCC3* expression. Spironolactone, which induces ERCC3 degradation, decreased LP-184 IC_{50} 3 to 6 fold and enhanced GBM xenograft antitumor responses.

Conclusions: These results establish LP-184 as a promising chemotherapeutic for GBM with enhanced efficacy in intrinsic or spironolactone-induced TC-NER–deficient tumors.

Introduction

Glioblastoma (GBM; WHO grade 4 astrocytoma) has an incidence of approximately 3 per 100,000 and accounts for approximately 60% of adult primary brain malignancies (1). Current best standard-of-care therapy for GBM consists of maximal surgical resection, fractionated radiotherapy with concurrent temozolomide followed by adjuvant temozolomide (2). All tumors eventually recur, and there is no effective chemotherapy for recurrent GBM. Personalized treatment strategies for targeting well-established oncogenic drivers and immunotherapeutics remain insufficiently effective for multiple reasons including poor CNS bioavailability, tumor molecular heterogeneity, and unique features of the GBM immunosuppressive microenvironment.

Chemotherapy for GBM is currently limited to the blood–brain barrier (BBB) permeable alkylating agents temozolomide and carmustine/lomustine (BCNU/CCNU). Temozolomide is a monofunctional SN1-alkylating agent. Temozolomide's most mutagenic and functionally important modification, O^6-methylguanine, is reversed by O^6-methylguanine-DNA methyltransferase (MGMT), rendering the majority of newly diagnosed and recurrent GBM resistant (3). MGMT activity is deficient in 30% to 40% of GBM due to transcriptional suppression by promoter DNA methylation and GBM patients with tumor *mgmt* methylation experience a corresponding approximate 12-month increase in survival (4). Temozolomide has limited efficacy against recurrent GBM for multiple reasons including MGMT reexpression and other resistance mechanisms (5–7). The nitrosoureas BCNU and CCNU are additional SN1-alkylating agents, and their utility is also compromised by similar resistance mechanisms and greater myelosuppression.

Alternative alkylating agents could have considerable efficacy as a general alternative to temozolomide, or in the specific context of temozolomide resistance. LP-184 is an alternative alkylating agent of the acylfulvene class that are prodrugs activated by oxidoreductases, especially PTGR1 (8). Acylfulvenes modify DNA by primarily alkylating adenine at the N^3-position not reported to be affected by MGMT (9–11). Instead, DNA damage by acylfulvenes is primarily repaired via transcription-coupled nucleotide excision repair (TC-NER) and homologous recombination (12–14). We have previously shown broad antitumor activity of LP-184 across 85 cell lines of various tumor types, including 7 conventional GBM lines maintained in serum-containing medium (15). On average, the IC_{50} of LP-184 in cancer lines was found to be 225 nmol/L, similar to that in the previously examined GBM lines (mean IC_{50} of 210 nmol/L), suggesting that LP-184 may be an effective alkylating agent for GBM assuming suitable pharmacodynamics. We now show efficacy of LP-184 in multiple additional GBM cell models including state-of-art

[1]Hugo W. Moser Research Institute at Kennedy Krieger, Baltimore, Maryland. [2]Lantern Pharma Inc., Dallas, Texas. [3]Department of Neurology, The Johns Hopkins University School of Medicine, Baltimore, Maryland. [4]Department of Pharmacology and Molecular Sciences, The Johns Hopkins University School of Medicine, Baltimore, Maryland. [5]Johns Hopkins Drug Discovery, The Johns Hopkins University School of Medicine, Baltimore, Maryland. [6]Department of Oncology, The Johns Hopkins University School of Medicine, Baltimore, Maryland.

Corresponding Author: John Laterra, The Kennedy Krieger Institute, 707 North Broadway, Baltimore, MD 21205. Phone: 443-923-2679; E-mail: laterra@kennedykrieger.org

Clin Cancer Res 2023;XX:XX–XX

doi: 10.1158/1078-0432.CCR-23-0673

Translational Relevance

Temozolomide, the most effective standard-of-care chemotherapy for newly diagnosed glioblastoma, is ineffective in approximately 70% of patients due to MGMT-driven resistance, and there is no effective chemotherapy for recurrent GBM. New agents with activity against temozolomide-resistant and recurrent GBM are desperately needed. We report multiple findings supporting the potential for LP-184, a novel alkylating agent with FDA orphan drug designation, to fill this void: (i) low nanomolar activity; (ii) favorable CNS penetration; (iii) durable regression of tumor xenografts and animal survival prolongation; (iv) synthetic lethality with nucleotide excision repair (NER) inhibition; and (v) transcriptomic/pathway predictors of LP-184 sensitivity in clinical GBM and GBM subsets. These laboratory-based findings and global unbiased clinical dataset analyses provide the foundation for testing LP-184 in patients with GBM and suggest enhanced efficacy against tumors with intrinsic or induced NER deficiency.

neurospheres and primary PDX-derived cell isolates. Pharmacokinetic studies showed that intravenous LP-184 reaches mouse brain and orthotopic GBM xenografts at concentrations well-above *in vitro* IC_{50} concentrations. We also present results from *in vivo* studies showing that systemic LP-184 induces the regression of GBM xenografts and prolongs survival of mice bearing preestablished orthotopic tumors and that cotreatment with spironolactone, a TC-NER inhibitor, sensitizes GBM cells and xenografts to LP-184. In addition, bioinformatic analyses have identified associations of a key signaling pathway (EGFR) and TC-NER genes (e.g., ERCC3) with predicted LP-184 sensitivity in clinical GBM samples. These findings identify LP-184 as a new promising chemotherapeutic agent for potential clinical translation in patients with GBM and other CNS malignancies.

Materials and Methods

Materials

LP-184 was provided by Lantern Pharma. Formic acid (98%, v/v in water) and acetonitrile (HPLC grade) were obtained from EMD Chemicals Inc. Deionized water was obtained from a Milli-Q-UF system (Millipore) and used for all aqueous solutions. NOD SCID mice were obtained from the Johns Hopkins breeding facility. Ncr-nu/nu mice were obtained from Charles River Laboratories. All other chemical reagents were purchased from Sigma-Aldrich.

Cell culture

The low passage patient-derived neurosphere line 612 and M1123 neurosphere line (kind gift from Dr. Ichiro Nakano, University of Alabama, Birmingham) were derived and characterized as previously described (16, 17). The patient-derived GBM xenograft line Mayo39 (*mgmt*-methylated/temozolomide-sensitive; refs. 18, 19) was obtained from the Mayo Clinic (19). Temozolomide-resistant Mayo39 cell variants (Mayo39-TMZR) were derived following prolonged culture with temozolomide. The 011310 PDX line was established from a GBM resected at Johns Hopkins Hospital. GBM neurospheres were maintained as spheres in serum-free conditions as described previously (20). U87, U251, LN-18, and low passage (<10) Mayo39, Mayo39-TMZR, and 011310 PDX-derived cells were maintained as monolayers in DMEM supplemented with 10% FBS (Thermo Fisher Scientific Inc.). All cells were grown at 37°C in a humidified incubator with 5% CO_2. All cell lines used in the study were tested for *Mycoplasma* and used within 20 passages of STR profiling.

Cell viability assays

In vitro cell viability was quantified by either MTT assay (Thermo Fisher, Catalog # M6494) or Cell Titer-Glo 2.0 assay (Promega Catalog #9241) as per the manufacturer's instructions. IC_{50}s were calculated using https://www.aatbio.com/tools/ic50-calculator. For cell death response, caspase activation was measured using the Caspase-Glo 3/7 Assay (Promega, Catalog #G8090). See Supplementary Materials and Methods for details.

In vitro BBB permeability assay

The human BBB model was obtained from Neuromics and the assay performed by Visikol, Inc., according to the manufacturer's specifications. See Supplementary Materials and Methods for details.

Tumor xenografts

All animal procedures were approved by the Johns Hopkins Animal Care and Use Committee. Xenografts were established as described previously (20). For subcutaneous xenografts, nude mice received 4×10^6 U87 or 1×10^6 M1123 cells suspending in 50 μL PBS containing Matrigel (Fisher Corning, Cat# CLS3471; 1:1) implanted to the dorsal upper thighs. Tumor volumes were quantified by [length (a) and width (b)] using $V = ab^2/2$[21]. For orthotopic xenografts, NOD SCID mice received 1×10^5 U87 or 2×10^4 M1123 cells suspended in 2 μL PBS to the right caudate/putamen. At the indicated postimplantation days, mice were treated with LP-184 (4 mg/kg i.v.) and/or spironolactone (Thermo Fisher catalog# 02605G; 25 mg/kg, i.p.) or vehicle only as indicated. Animals with orthotopic tumors were sacrificed at the indicated times and tumor sizes quantified by computer-based morphometric analysis as described previously (20). See Supplementary Materials for more details.

Pharmacokinetics in tumor-bearing mice

Briefly, mice ($n = 3$/time point) received 4 mg/kg LP-184 via tail vein injection (i.v.) and sacrificed at the indicated times for plasma and tissue collection. To quantify LP-184, methanol containing 0.5 μmol/L losartan was added to preweighed tissue samples as an internal standard. Plasma or tissue homogenates from untreated animals were spiked with LP-184 from 3×10^4 to 3 ng/g or ng/mL to generate a standard curve. Samples were analyzed on a Vanquish UHPLC coupled to an Altis triple quadrupole mass spectrometer (Thermo Fisher Scientific Inc.) and separated on an Agilent EclipsePlus C18 RRHD (1.8 μm) 2.1 × 100 mm column. Peaks were quantified with Xcalibur software version 4.2.47 (Thermo, RRID:SCR_014593). See Supplementary Methods for details.

Bioinformatic analyses

Machine learning predictions used RNA-seq expression data and a random forest LP-184 model as described previously (15). To make predictions, the LP-184 model requires 10 genes in $\log_2+1$ FPKM format: *PTGR1, AGRN, PRR3, HOXA3, BCOR, CBX2, PLOD2, ACVR2B, RAB2A*, and *S100A10*. Expression values are normalized sample-wise prior to predictions. The model predictions were in the form of $-\log_{10} IC_{50}$ molar values in a standard score format assessable either as a continuous quantitative prediction of IC_{50}, or in a relative manner, for example, as sensitive or resistant compared to the average IC_{50}s in the training set. The machine learning model was trained using 62 samples from both tumor cell lines and PDX *ex vivo* models having RNA-seq data and matching LP-184 IC_{50} values, which

included 5 brain tumor lines including 1 lower grade glioma and 3 derived from GBM specimens. RNA-seq data of cell lines were downloaded from CellMinerCDB (https://discover.nci.nih.gov/rsconnect/cellminercdb), CCLE (https://portals.broadinstitute.org/ccle/data), and GEO for the GBM1B neurosphere line (GSE151995).

Clinical analysis used TCGA data downloaded from XenaBrowser (https://xenabrowser.net/datapages/) after RNA-seq were processed and used for machine learning predictions as described previously (15). Predictions were used to conduct gene set enrichment analysis (GSEA) correlating gene expression to predicted LP-184 response, where a higher LP-184 response indicated greater sensitivity. Correlation-ranked genes were used as input for the fgsea R package to identify the top-10 (based on *P* value) positively and negatively associated biological pathways in the Reactome (RRID:SCR_003485), WikiPathways, and KEGG (RRID:SCR_012773) databases. GSEA was performed with parameter settings of 500 permutations and a maximum pathway size of 500. Molecular and histologic subtypes of the TCGA GBM cohort were downloaded from the TCGA Portal (tumorsurvival.org/index.html) and matched to expression data using the tumor sample barcode. Expression data for normal brain were downloaded from GTEx data included in the TCGA-TARGET dataset.

Immunoblotting

Immunoblotting was performed as described previously (20) using NOVEX 4% to 12% Tris-glycine gradient gels (Thermo Scientific) and Amersham Protran nitrocellulose membranes (GE HealthCare). Membranes were probed with primary antibodies for ERCC3 (Aviva System Biology, ARP37963_P050, RRID:AB_10713125), phosphogammaH2AX (Cell Signaling, #2577S), GAPDH (Santa Cruz Biotechnology, #sc-47724, RRIDAB_627678), MGMT (Santa Cruz Biotechnology #sc-166528, RRID:AB_2250597) or actin (Cell Signaling cat #3700S), and secondary antibodies labeled with IRDye infrared dye (LI-COR Biosciences). Protein band intensities were quantified using the Odyssey Infrared Imager (LI-COR Biosciences) and analyzed using the Image Studio acquisition software from LI-COR imaging systems.

Statistical analysis

All *in vitro* experiments were performed using $n \geq 3$ and repeated at least twice in each cell model. PRISM GraphPad 9 (RRID:SCR_002798) was used for statistical analyses. Two group comparisons were analyzed for variation and significance using a two-tailed, type 1 *t* test. One-way or two-way ANOVA and Tukey or Bonferroni *post hoc* tests were used when comparing multiple variables. Survival data were compiled using Kaplan–Meier methodology. *P* values lower than 0.05 were considered statistically significant.

Data and material availability

The data supporting this study are available within the paper and its Supplementary Data file. All other data are available from the authors upon reasonable request.

Results

GBM cell sensitivity to LP-184 *in vitro*

LP-184 activity against GBM was previously suggested by above-average sensitivity in a screen of NCI60 cell lines to LP-184, a purely negative stereoisomer of hydroxyureamethylacylfulvene (**Fig. 1A**; ref. 15). Multiple complementary GBM cell models were evaluated for sensitivity to LP-184 *in vitro* (**Fig. 1B–D**). U87 cells (hypermethylated *mgmt* and temozolomide sensitive; ref. 6), mesenchymal GBM-derived neurospheres M1123, a low passage GBM derived neurosphere isolate GBM612 and primary cells derived from the hypermethylated *mgmt*/TMZ sensitive Mayo39 PDX model (18) were also sensitive with IC_{50}s ≤ 300 nmol/L. The MGMT-expressing LN-18 cell line (21) and Mayo39-TMZR PDX-derived cells and MGMT-negative 11310 neurosphere cells were temozolomide-resistant (IC_{50} > 500–1,000 μmol/L) and highly sensitive to LP-184 (IC_{50} = ∼20–210 nmol/L). LP-184 was found to induce DNA damage responses within 12- to 24 hours of cell exposure and prior to effects on cell viability and apoptotic cell death (i.e., caspase activation) detected at 48 hours of exposure (**Fig. 1E–G**). LP-184 dramatically depleted GBM neurospheres of their stem-like cells and inhibited their clonogenic growth (**Fig. 1H**). These results show that LP-184 induces DNA damage with low nanomolar range cytotoxicity to GBM cells and that neither temozolomide resistance nor MGMT expression predict cross resistance to LP-184.

LP-184 pharmacokinetics and CNS bioavailability

Analysis using admetSAR2, an *in silico* tool for predicting the ADME (absorption, distribution, metabolism, and excretion) properties of compounds (22), predicted a 0.97 probability of BBB permeability for LP-184, similar to the 0.99 probability predicted for current standard-of-care temozolomide. BBB permeability was further evaluated using an *in vitro* BBB model consisting of brain endothelial cells, pericytes, and astrocytes (Supplementary Fig. S1A). The apparent permeability of LP-184 at 30 minutes was 1.54E−04 cm/s compared with 1.72E−04 cm/s for temozolomide (Supplementary Fig. S1B). Viability of cells in the barrier was >95%, indicating permeability was not a result of damage to the cellular layer (Supplementary Fig. S1C).

Systemic and brain pharmacokinetics was quantified in mice bearing orthotopic M1123 tumor xenografts following a single tail vein bolus of LP-184 (4 mg/kg), a dose subsequently used for therapeutic experiments (**Fig. 2**, top). The half-life ($T_{1/2}$) was 0.24 hour and LP-184 achieved a C_{max} of 11,296 nmol/L in plasma and 2,539 nmol/L in tumor at 5 minutes. C_{max} for peritumoral and contralateral brain were 916 and 732 nmol/L, respectively, at 15 minutes (**Fig. 2**, bottom). The overall exposures in plasma (AUC_{plasma}), tumor (AUC_{Tumor}), peritumoral brain ($AUC_{Peritumoral\ Brain}$), and contralateral brain ($AUC_{Contralateral\ Brain}$) were calculated to be 1,592, 319, 165, 123 ng/h/g respectively. The tumor, peritumoral brain, and contralateral brain penetration indices were $AUC_{Tumor/Plasma} = 0.2$, $AUC_{Peritumoral\ Brain/Plasma} = 0.103$ and $AUC_{Contralateral\ Brain/Plasma} = 0.077$, respectively. Thus, tumor/plasma ratio was 2-fold higher compared with brain/plasma ratio. Tumor C_{max} was 2.7-fold higher than in the peritumoral brain and 3.5-fold higher than the contralateral brain. Maximum brain and brain tumor concentrations following a single intravenous bolus were well above the IC_{50} (∼46–300 nmol/L) for GBM cell lines, neurosphere lines and PDX-derived cell isolates (**Figs. 1B** and **2B**).

GBM xenograft responses to LP-184

Nude mice bearing preestablished subcutaneous xenografts derived from either mesenchymal M1123 GBM neurosphere cells or U87 cells received LP-184 (4 mg/kg i.v. q.o.d × 4) beginning when tumors measured approximately 100 mm^3. Tumor regressions were observed in both models beginning as early as posttreatment day 2 with either complete regression or halted tumor growth in all animals (**Fig. 3A–C**). Tumor responses were highly statistically significant ($P < 0.0001$).

Efficacy was also examined in animals bearing preestablished orthotopic tumor xenografts (**Fig. 4**). Tumor cells were implanted to the right caudate-putamen of NOD SCID mice. Animals received LP-184 (4 mg/kg i.v. q.o.d × 4) beginning on postimplantation day 8 for

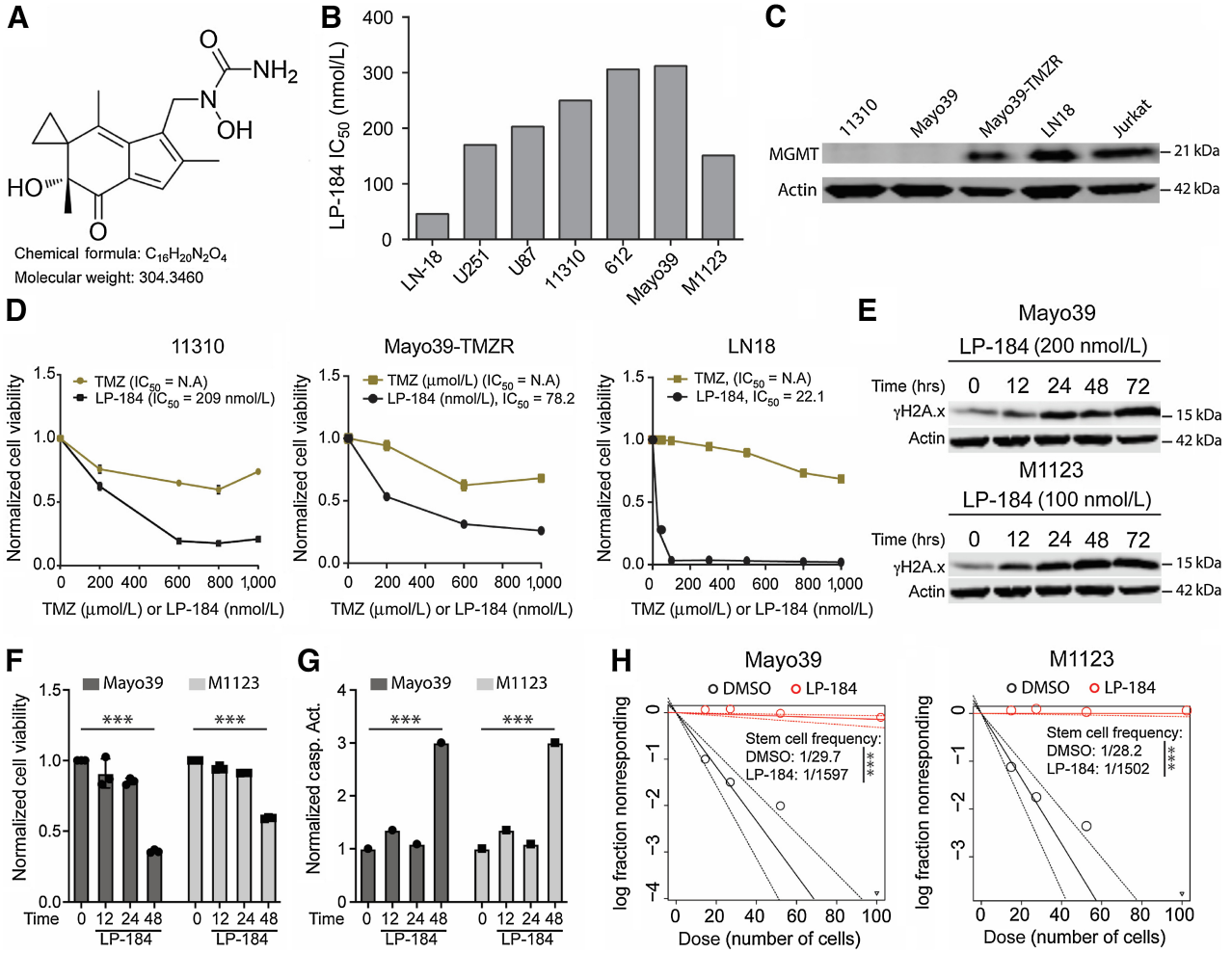

Figure 1.

LP-184 inhibits GBM cell viability. **A,** Chemical structure of the acylfulvene class small-molecule LP-184 (hydroxyureamethylacylfulvene). **B,** LP-184 nanomolar potency against multiple glioblastoma cell lines and isolates *in vitro*. **C,** Immunoblot showing MGMT expression in GBM cells and Jurkat cells as positive control. **D,** LP-184 nanomolar potency against MGMT-expressing and MGMT-negative temozolomide-resistant GBM cells. **E,** Immunoblot showing temporal DNA damage response in GBM cells treated with LP-184. **F,** Viability of Mayo39 and M1123 cells treated with LP-184 (200 and 100 nmol/L, respectively). **G,** Caspase activation in Mayo39 and M1123 cells treated with LP-184 (200 and 100 nmol/L, respectively). **H,** Inhibition of GBM stem-like cell clonogenic proliferation as determined by limiting dilution neurosphere assay. Mayo39 and M1123 neurospheres treated with 200 and 100 nmol/L LP-184, respectively. Cell viability in relative luminescence units (RLU). Data, mean ± SEM.

M1123 tumors and postimplantation day 17 for U87 tumors. A single cycle of LP-184 increased survival of animals with M1123 and U87 tumor xenografts by 22% (5.5 days, $P < 0.01$) and 24% (8 days, $P < 0.001$), respectively (**Fig. 4A** and **B**). Analysis of brains from animals randomly selected for sacrifice 4 days after completion of therapy showed that LP-184 reduced M1123 and U87 tumor burden by 90% ($P < 0.01$) and 75% ($P < 0.0001$), respectively (**Fig. 4C** and **D**). Each cycle of LP-184 was associated with various degrees of transient weight loss that stabilized or recovered after completing therapy (Supplementary Fig. S3).

Gene expression and pathway biomarkers of LP-184 sensitivity

We identified a 10-gene expression signature for LP-184 cell sensitivity by applying RADR (Response Algorithm for Drug positioning and Rescue), a machine learning–based gene expression signature platform, and a Random-Forest algorithm to the LP-184 IC_{50} results from 62 cell samples (i.e., NCI60, CCLE, PDXs) as described previously (15) and in Materials and Methods. This analysis accurately predicted in vitro GBM sensitivity to LP-184 (Pearson's Correlation Coefficient R = 0.99; **Fig. 5A**). Prostaglandin reductase 1 (PTGR1) expression was most highly associated with LP-184 sensitivity (Supplementary Fig. S3A), consistent with the known role for alkenal/one oxidoreductases in activating the similar acylfulvene drug, Irofulven (9). We therefore surveyed *PTGR1* expression levels in publicly available tumor RNA-seq samples from GBM patients. Using PTGR1 RNA-seq $\log_2$ FPKM data normalized for batch effects by the TCGA TARGET GTEx project, we found PTGR1 to be significantly (Wilcoxon $P < 2.2e{-}16$) elevated in GBM compared with normal brain (**Fig. 5B**). Consistently, we found that the same datasets harmonized by the GEPIA2 project had approximately 1.77-fold higher expression in GBM compared with normal brain (Supplementary Fig. S3B). These findings further support GBM as a target indication

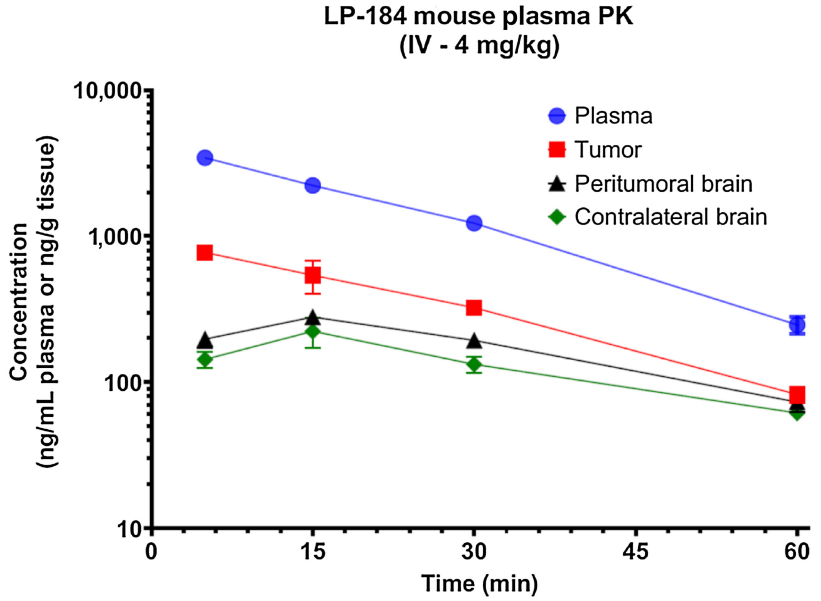

Measured analyte & dose	Matrix	Dosing route	Pharmacokinetic data (mean ± SEM)				Tissue/ plasma ratio
			C_{max} (ng/g or ng/mL)	T_{max} (h)	AUC_{0-t} (ng.h/g or ng.h/mL)	Half-life (h)	
LP-184 4 mg/kg	Plasma	IV	3,438 ± 125	0.0833	1,592 ± 48.7	0.236	–
	Peritumoral brain		279 ± 20.2	0.250	165 ± 11.6	0.383	0.103
	Contralateral brain		223 ± 50.6	0.250	123 ± 15.9	0.444	0.077
	Tumor		773 ± 58.6	0.0833	319 ± 36.4	0.281	0.200

Figure 2.
LP-184 pharmacokinetics and CNS bioavailability. Top, LP-184 concentration–time curve in mouse plasma, brain, and brain tumor tissues following a single intravenous bolus (4 mg/kg). bottom, *In vivo* pharmacokinetics parameters following a single intravenous bolus (4 mg/kg). Data, mean ± SEM ($n = 3$).

for LP-184 therapy. Analysis of PTGR1 expression in astroglioma subtypes identified highest expression in mesenchymal GBM compared with classical and proneural GBM subtypes and lowest expression in G-CIMP glioma, which associated with predicted IC_{50}s by the machine learning model (Supplementary Fig. S3C). Furthermore, genes differentially expressed in GBM showed significant ($P < 0.05$) multi-omic parameter correlations with predicted LP-184 sensitivity. Genes including MGMT, LPAR, LAMB1, and UGDH are often upregulated in GBM and associated with temozolomide resistance (23) and such upregulation positively

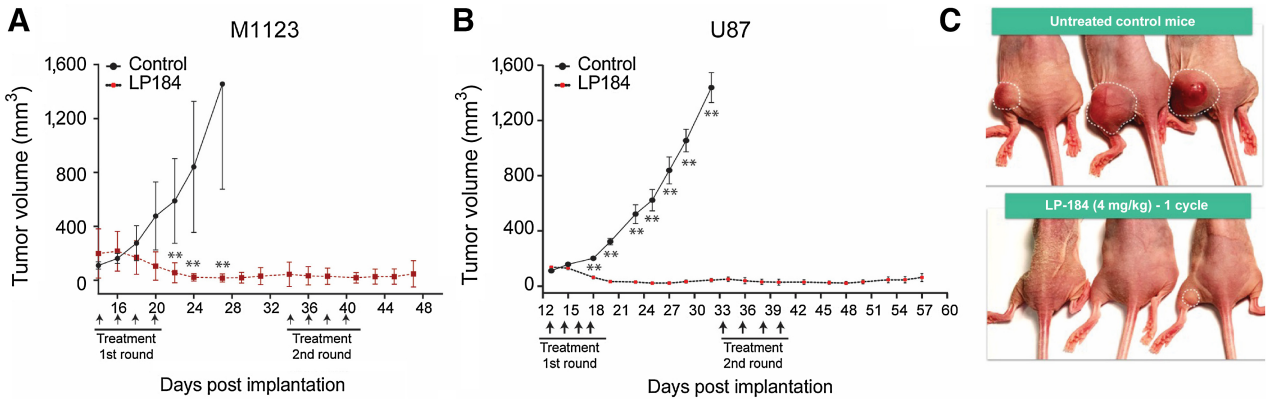

Figure 3.
LP-184 induces regression of subcutaneous GBM xenografts. Mice with subcutaneous tumor xenografts received LP-184 (4 mg/kg i.v.) or vehicle as indicated by arrows. Tumor volumes were calculated as in Materials and Methods. **A,** Mesenchymal M1123 PDX xenografts. $n = 3$ for control, $n = 4$ for LP-184–treated mice. **B,** U87 xenografts. $n = 5$ for control, $n = 10$ for LP-184–treated mice. **C,** Representative images of control and LP-184–treated M1123 tumor xenografts. Data, mean ± SEM.

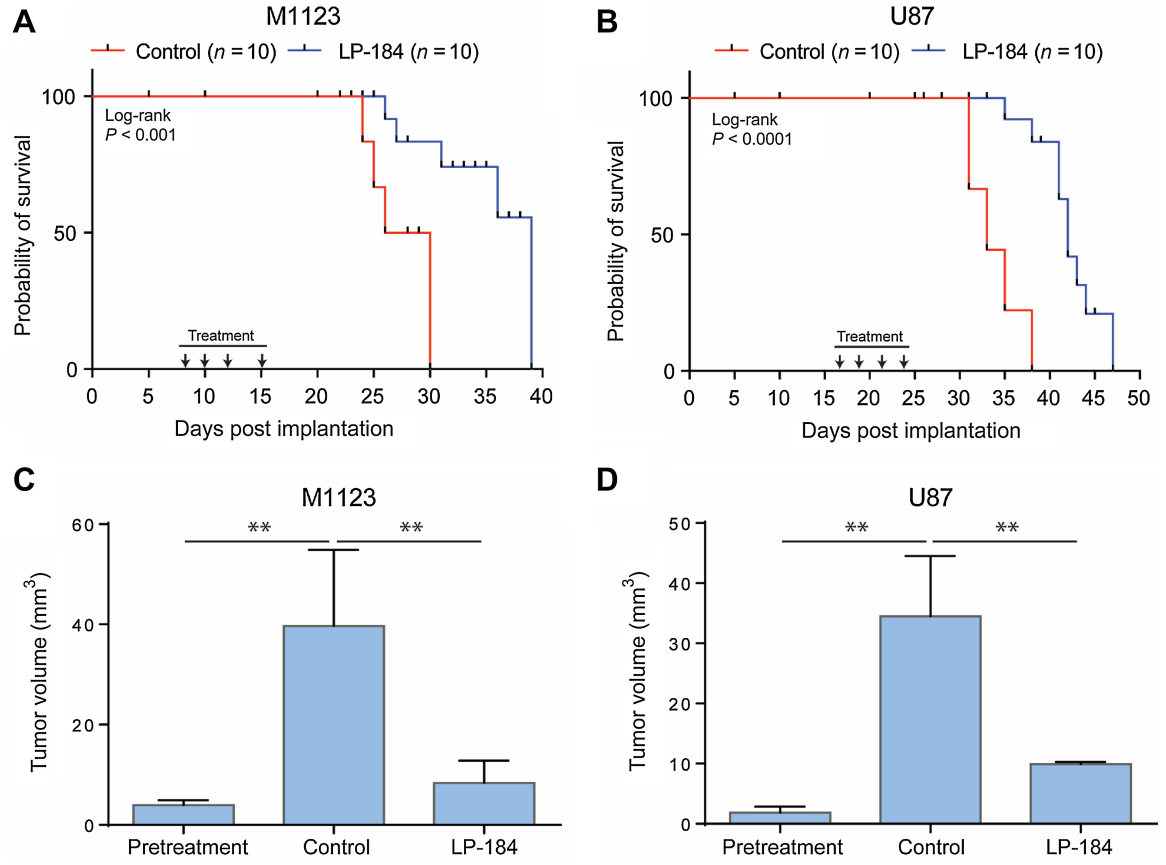

Figure 4.

LP-184 prolongs survival of mice with orthotopic GBM xenografts. Mice with orthotopic M1123 or U87 xenografts received vehicle or LP-184 (4 mg/kg i.v.) on days indicated by arrows. Five mice were randomly selected and sacrificed immediately prior to starting treatments and five mice from control and LP-184 treatment groups were randomly selected and sacrificed following the last infusion for histopathologic assessment of tumor volumes pretreatment and posttreatment. The remaining mice ($n = 10$) were evaluated for survival (**A** and **B**). **C,** M1123 tumor volumes pretreatment (postimplantation day 8) and on postimplantation day 16. **D,** U87 tumor volumes pretreatment (postimplantation day 16) and on postimplantation day 25. Tumor volumes, mean ± SEM.

correlated with LP-184 sensitivity, translating into potential superiority of LP-184 in such tumors. Similarly, genes including MCM6, PCMT1, CYFIP2, and HIST3H2A reported to be downregulated in GBM and associated with temozolomide resistance (23) correlated negatively with predicted LP-184 sensitivity, and thus suggest potential benefit of LP-184 in such tumors. Interestingly, EGFR, ANXA2, DOCK1, and S100A11 (24–27) represent an overlap between a gene expression profile underlying GBM tumorigenesis and a gene expression profile that supports heightened sensitivity to LP-184. (Supplementary Tables S1–S3).

High sensitivity to LP-184 was statistically significantly associated with lower DNA damage repair enrichment (i.e., negative normalized enrichment score) and associated with higher expression of oncogenic pathway drivers in GBM, including EGFR and MAPK (i.e., positive normalized enrichment score; **Fig. 5C**). GSEA reactome pathways showed DNA repair in the top 10 lowest normalized enrichment scores to LP-184 response (Supplementary Fig. S2D). In an analysis of key DNA repair genes potentially involved in sensitivity predictions, expression of the TC-NER gene *ERCC3* had the highest correlation with predicted LP-184 IC_{50}s (**Fig. 5D**). LP-184 predicted IC_{50}s were significantly higher in TCGA GBM samples with above-average *ERCC3* expression (**Fig. 5E**). ERCC3/XBP is a helicase in the TFIIH complex involved in unwinding of DNA at lesions to facilitate TC-NER (28).

NER inhibition sensitizes GBM cells and xenografts to LP-184

To validate the predicted impact of *ERCC3* expression on GBM resistance, we asked if ERCC3 inhibition sensitizes GBM to LP-184. Spironolactone (SP) is a BBB permeable aldosterone antagonist that inhibits TC-NER by inducing ubiquitin-mediated proteolytic degradation of ERCC3 (29–31). SP (25 μmol/L) treatment depleted GBM cells of ERCC3 protein by up to 95% (**Fig. 6A**). Treating GBM cells with SP increased the gamma-H2AX DNA damage response to LP-184 (**Fig. 6B**) and decreased LP-184 IC_{50} 3 to 6 fold (**Fig. 6C**). Animals with subcutaneous U87 xenografts were treated with SP alone, LP-184 alone, or their combination (**Fig. 6D**). SP monotherapy had no effect on tumor growth compared with vehicle-treated controls. LP-184 alone and combined with SP induced complete or near complete tumor regression. Beginning on ∼PID 25, tumor growth reemerged in 5 of 5 animals treated with LP-184 alone. Combining SP with LP-184 generated greater and more durable responses with tumor recurrence in only 1 of 5 animals (**Fig. 6D** and **E**). SP also sensitized aggressive orthotopic mesenchymal M1123 xenografts to LP-184 (**Fig. 6F**).

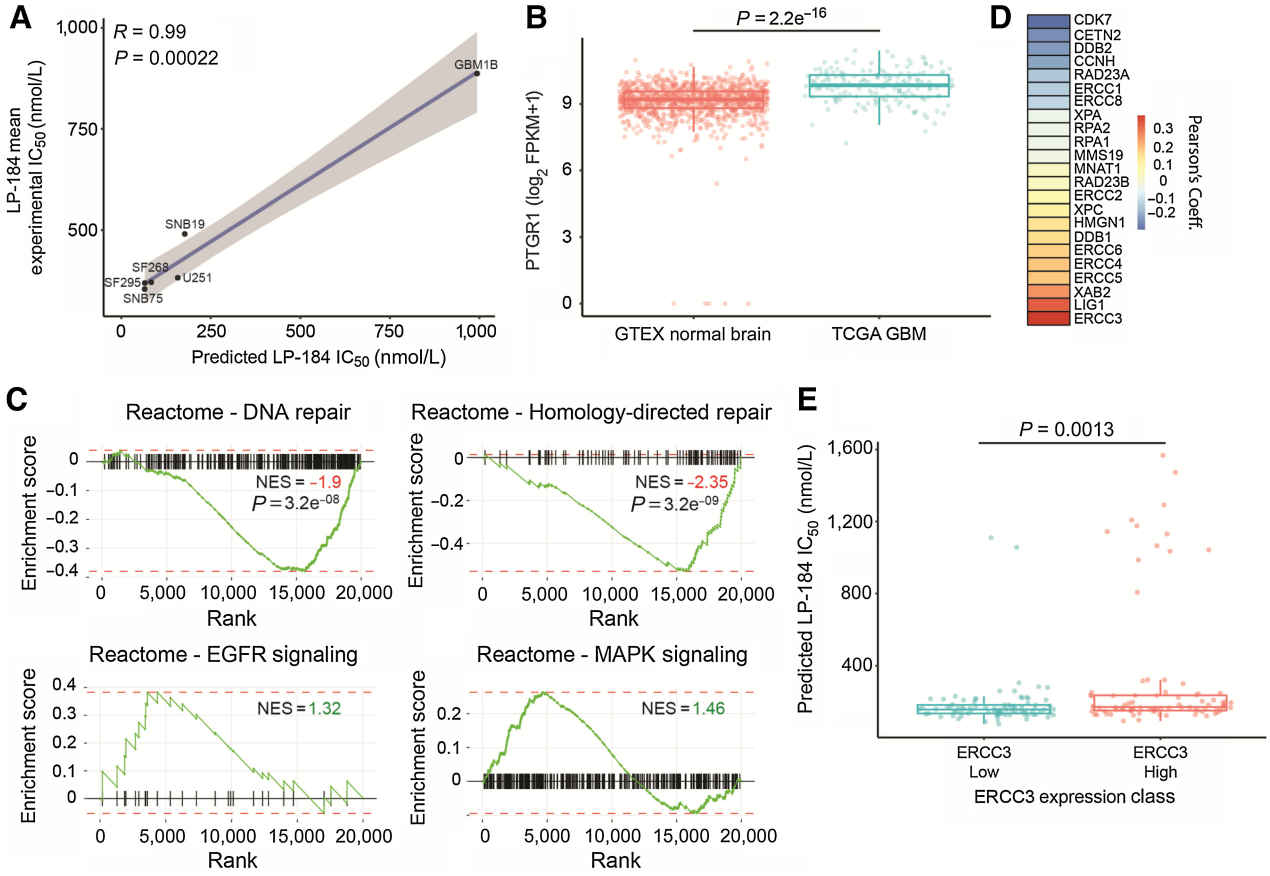

Figure 5.

Gene expression and pathway biomarkers of LP-184 sensitivity. **A,** Pearson correlation plot between experimental and predicted LP-184 IC_{50}s in GBM cell lines with full transcriptomic profiles available. **B,** PTGR1 RNA-seq expression in TCGA-GBM versus GTEX normal brain, normalized by the TCGA TARGET GTEX project. **C,** Gene set enrichment analysis of reactome pathways based on ranked expression derived from Pearson correlations of predicted IC_{50} and gene expression in TCGA GBM data. Subtitles indicates normalized enrichment score. **D,** Correlation of expression of Transcriptome-Coupled Nucleotide Excision Repair (TC-NER) genes and predicted LP-184 IC_{50}. ERCC3 expression most significantly contributes to high LP-184 IC_{50} in GBM. Blue colors represent negative correlations to predicted LP-184 $-\log_{10}$ IC_{50}s. **E,** TCGA GBM clinical samples with lower ERCC3 expression have greater predicted LP-184 sensitivity. Samples were divided into groups with ERCC3 expression above the mean (ERCC3 high) or below the mean (ERCC3 low).

Discussion

Recent advances are expanding the personalized therapeutic armamentarium for rare, molecularly distinct GBM subsets (e.g., BRAFV600E, NTRK1, and FGFR1 fusions). Otherwise, there have been no substantive advances in GBM chemotherapy since 2005 when temozolomide became standard-of-care for newly diagnosed GBM (32). This is a major roadblock to patient care since 60% to 70% of newly diagnosed GBM are inherently resistant to temozolomide and recurrent tumors acquire temozolomide resistance via multiple mechanisms (33). Attempts to reverse temozolomide resistance have been unsuccessful pointing to the need to identify new chemotherapeutic agents. One such agent undergoing clinical investigation is dianhydrogalactitol (VAL-083), an hexitol epoxide believed to methylate DNA at N^7-guanine, thereby rendering VAL-083 insensitive to MGMT expression (NCT02717962, NCT03970447). Pharmacokinetic studies for VAL-083 have demonstrated brain tumor/plasma and normal white matter/plasma ratios to be 1.3 and 0.3 (34). Despite this favorable BBB permeability profile, typical peak plasma concentrations were found to be 3.9 to 6.2 μmol/L compared with cytotoxic concentrations against GBM cells *in vitro* in the ∼5 μmol/L range (35, 36), suggesting that drug delivery to infiltrating tumor cells may be below that required for effective *in vivo* cytotoxicity. More recently, novel medicinal chemistry approaches have been used to generate temozolomide derivatives with preclinical activity in temozolomide-resistant GBM cells and xenografts (33).

Our current *in vitro* and *in vivo* results identify the acylfulvene derivative LP-184 as a promising alkylating agent for GBM, including temozolomide-resistant GBM. Our preclinical findings show that LP-184 fulfills multiple requirements for clinical translation against infiltrating CNS malignancies such as GBM (37). Results using multiple GBM cell lines and primary isolates show IC_{50}s in the ∼22–300 nmol/L range including sensitivity against MGMT-expressing and MGMT-negative temozolomide-resistant cells. These *in vitro* findings translated *in vivo* as evidenced by durable regression of subcutaneous GBM xenografts and survival prolongation in animals with orthotopic GBM xenografts including those derived from aggressive mesenchymal GBM neurospheres. Tumor responses to LP-184 were found to be substantially more robust and durable than those initially reported for temozolomide in a similar *in vivo* model (38). Pharmacokinetics in

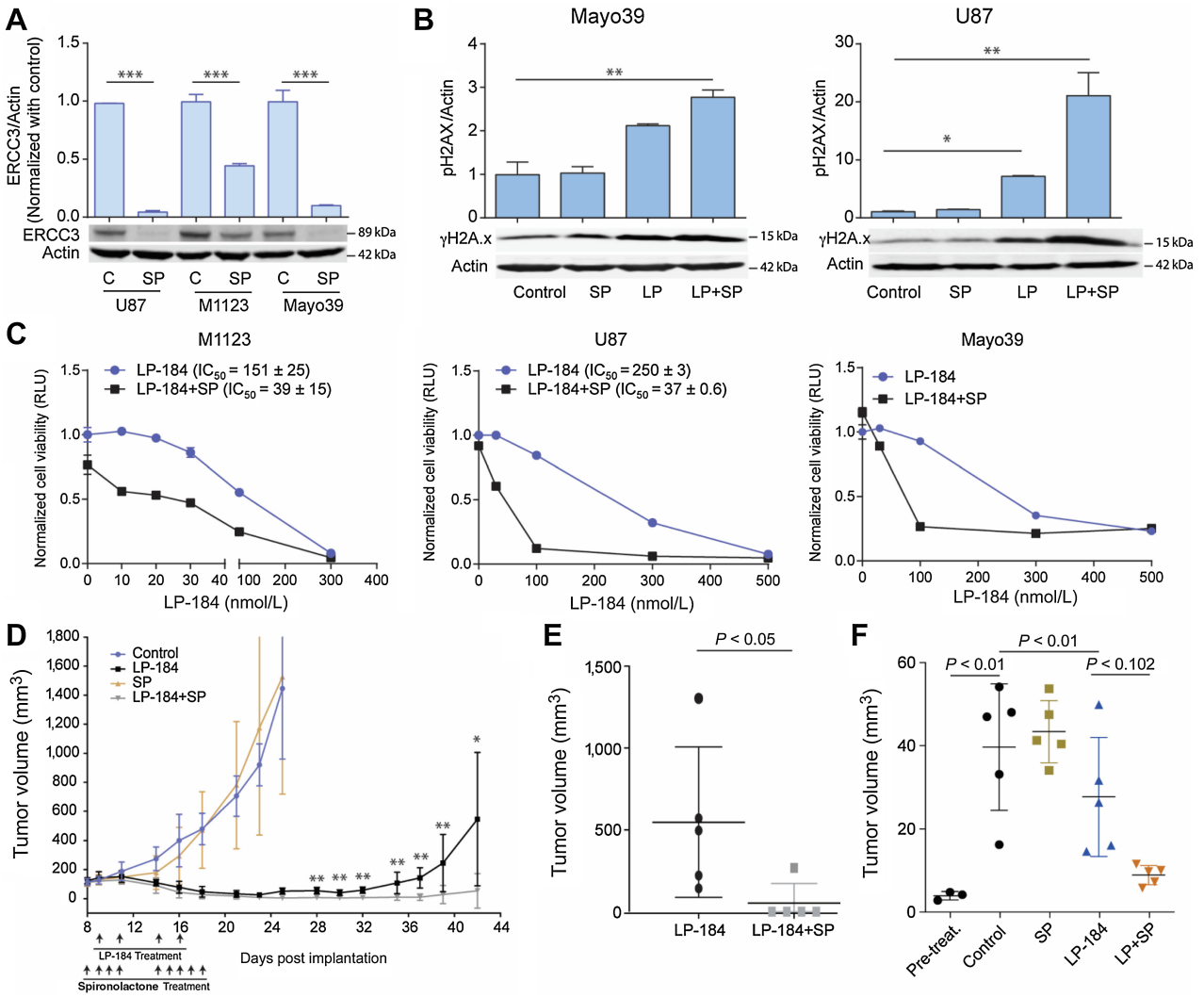

Figure 6.

Spironolactone sensitizes GBM cells and xenografts to LP-184. **A,** Immunoblot showing ERCC3 protein depletion in GBM cells treated with spironolactone (25 μmol/L). **B,** Immunoblot showing that spironolactone (SP) amplifies the DNA damage response (i.e., phospho-γH2AX induction) to LP-184 in GBM cells. **C,** Effect of combining spironolactone (25 μmol/L) with LP-184 (treatment for 72 hours) on GBM cell viability. M1123 cells adherent on laminin coated plates in neurosphere medium. U87 cells adherent in 0.1% serum. Relative cell viability determined by Cell Titer Glow assay. **D,** Mice with subcutaneous U87 tumor xenografts were treated with vehicle, spironolactone alone (25 mg/kg i.p.), LP-184 alone (4 mg/kg i.v.) or LP-184 + spironolactone as indicated by arrows. Line plots show tumor volumes versus time ($n = 5$). **E,** Scatter plot shows sizes of individual tumors at end of experiment shown in **D** on postimplantation day 42. **F,** Mice with orthotopic M1123 xenografts were treated with either SP alone (25 mg/kg i.p, on postimplantation days 7–12), LP-184 alone (4 mg/kg i.p. on postimplantation days 8, 10, 12), SP + LP-184, or vehicle only as control. Scatter plot shows tumor sizes before treatment start (PID 8) and following treatment (PID 13). Data for **A** to **D**, mean ± SEM.

normal and tumor-bearing mice revealed effective CNS availability to tumor core ($C_{max} \sim 2{,}500$ nmol/L), peritumoral brain ($C_{max} \sim 900$ nmol/L), and normal brain ($C_{max} \sim 730$ nmol/L) where infiltrating tumor cells reside behind a relatively intact BBB. Subcutaneous tumor xenografts appeared to respond more robustly to LP-184 compared with orthotopic xenografts, suggesting differential drug exposure despite the relatively favorable CNS penetration. Alternate explanations include differences in tumor microenvironments and the different dosing regimens used (two treatment cycles for subcutaneous models vs. one cycle for orthotopic models).

LP-184 is a prodrug converted to an active alkylating agent by the enzyme prostaglandin reductase 1 (PTGR1). Machine learning has recently been applied to predict drug responses based on molecular features, such as gene expression, DNA methylation, or genomic mutations (39–41), and we previously published a 16-gene XGBoost-algorithm model that predicted the response to LP-184 in 2D cell lines (15). Here, we developed a new Random forest algorithm LP-184 predictive model that was trained with 10 RNA-seq expression features, using data from cell lines and PDX of multiple cancers, including GBM. This model demonstrated decreased error in blind validation set predictions, and similar to the XGBoost model was most strongly influenced by PTGR1 expression. Model predictions of GBM samples tested in this study had a 0.99 Pearsons correlation to measured drug response. Such

machine learning model predictions have potential utility in patient stratification based on tumor gene expression measurements, as well as the evaluation of the cancer types and subtypes as candidate indications. The power for PTGR1 expression to predict LP-184 sensitivity likely results from PTGR1's role in converting LP-184 to its active metabolite that cannot be practically measured in therapeutic settings due to its extreme lability. Hence, PTGR1 has the potential to be an invaluable biomarker for identifying tumor sensitivity, predicting rates of drug conversion and dissecting resistance mechanisms.

Multiple findings from transcriptomic and machine-learning analyses of tumor cell line and clinical specimen datasets point to GBM as a promising target for LP-184 therapeutics. Acylfulvenes are prodrugs activated by oxidoreductases and expression of the oxidoreductase PTGR1was found to be upregulated in clinical GBM samples and strongly predict tumor cell sensitivity to LP-184. High GSEA scores for EGFR signaling, oncogenic pathways associated with the majority of GBM (42), also predicted sensitivity to LP-184. In contrast, MGMT status was not found to predict LP-184 sensitivity, a prediction validated by our experimental results showing LP-184 sensitivity in MGMT-expressing and temozolomide-resistant GBM cells. Ultimately finding that LP-184 is active against temozolomide-resistant GBM in the clinical setting would significantly advance treatment options for most patients. DNA damage induced by acylfulvenes is reported to be repaired by TC-NER. Low GSEA scores for DDR and low expression of the TC-NER gene *ERCC3* significantly associated with LP-184 sensitivity. ERRC3/XPB functions as an ATP-dependent helicase. ERCC3 is a critical component of the TC-NER protein complex and provides functions critical for TC-NER dependent DNA repair (28). A role for TC-NER in protecting GBM cells from LP-184 was validated by our finding that spironolactone, which inhibits TC-NER by inducing ERCC3 proteolytic degradation (8, 37), sensitizes GBM cells and xenografts to LP-184. Spironolactone has also been found to upregulate NKG2D ligands on tumor cells and thereby enhance NK-dependent tumor cell lysis (43). While this activity could be an additional advantage in the clinical setting, it would not explain the capacity for spironolactone to reduce LP-184 IC_{50} *in vitro* and would not likely have such dramatic effects on tumor xenograft responses to LP-184 in our immunosuppressed animals.

A promising strategy to exploit the synthetic lethality potential of DNA-damaging agents is to combine them with alternative inhibitors of the DNA damage repair (DDR) machinery, such as inhibitors for poly(ADP-ribose) polymerase (PARP). PARP inhibitors (PARPis) have received regulatory approval for breast, ovarian, prostate, and pancreatic cancer treatment based on biomarker-dependent efficacy profiles. In these cancer types, patients carrying specific mutations in BRCA1/2 have shown better antitumor response to PARPis compared with wild-type carriers. Mutated BRCA genes are infrequent in GBM, but other genetic alterations can lead to the same phenotype collectively referred to as "BRCAness". The most promising biomarkers of BRCAness in GBM include IDH1/2, EGFR, PTEN, MYC, ERβ, RAD51, ATM, ATR, KDM4A, KDM4B, and PRKDC (44). Twenty percent to 35% of GBM can potentially be classified under BRCAness phenotype based on this panel of biomarkers (45). BRCAness status identified by accurate biomarkers can ultimately predict responsiveness to PARPi therapy and the capacity for PARPi to sensitize IDH-mutant gliomas is currently being tested clinically (NCT03914742; ref. 46). We have also observed that LP-184 is highly effective in homologous recombination–deficient tumors such as breast cancers (unpublished findings). It remains possible that part of the efficacy of LP184 in GBM is realized by the BRCAness of GBM. This suggests the potential efficacy of a combination therapy approach involving LP-184 and PARPi in patient subsets based on gene expression and mutation correlates of LP-184 sensitivity and GBM BRCAness.

Our study identifies LP-184 as a promising chemotherapeutic with clinical translation potential for treating patients with GBM. Our results indicate that GBM sensitivity to LP-184 is not likely to be influenced by temozolomide resistance. Clinically relevant patient subpopulations defined by elevated activity in EGFR or AKT signaling or endogenous deficiencies in the TC-NER function are predicted to be particularly responsive to LP-184. ERCC3 levels may serve as a key biomarker guiding LP-184 use and spironolactone, a well-tolerated FDA-approved BBB-permeable diuretic, could serve as an adjunct to enhancing LP-184 clinical efficacy.

Authors' Disclosures

A. Kulkarni reports other support from Lantern Pharma outside the submitted work. R. Rais reports other support from Lantern Pharma during the conduct of the study. J. Zhou reports personal fees from Lantern Pharma, Inc. outside the submitted work, is a salaried employee of the pharmaceutical company Lantern Pharma, Inc., holds options to purchase common stock of Lantern Pharma Inc., and may be included as an inventor on patent applications filed by Lantern Pharma Inc. B.S. Slusher reports grants from Lantern Pharma Inc., during the conduct of the study. K. Bhatia reports other support from Lantern Pharma during the conduct of the study, other support from Lantern Pharma outside the submitted work, as well as a patent for Method of Use pending. J. Laterra reports grants from Lantern Pharma, Inc., during the conduct of the study. No disclosures were reported by the other authors.

Authors' Contributions

B. Lal: Data curation, formal analysis, investigation, writing–review and editing. **A. Kulkarni:** Conceptualization, data curation, writing–review and editing. **J. McDermott:** Data curation, formal analysis, writing–review and editing. **R. Rais:** Data curation, formal analysis, investigation, writing–review and editing. **J. Alt:** Investigation. **Y. Wu:** Investigation. **H. Lopez-Bertoni:** Supervision, methodology, writing–review and editing. **S. Sall:** Data curation. **U. Kathad:** Data curation, investigation, methodology. **J. Zhou:** Data curation, investigation. **B.S. Slusher:** Methodology. **K. Bhatia:** Conceptualization, writing–review and editing. **J. Laterra:** Conceptualization, formal analysis, supervision, funding acquisition, writing–original draft, writing–review and editing.

The publication costs of this article were defrayed in part by the payment of publication fees. Therefore, and solely to indicate this fact, this article is hereby marked "advertisement" in accordance with 18 USC section 1734.

Note

Supplementary data for this article are available at Clinical Cancer Research Online (http://clincancerres.aacrjournals.org/).

Received March 3, 2023; revised June 15, 2023; accepted July 24, 2023; published first July 26, 2023.

References

1. Batash R, Asna N, Schaffer P, Francis N, Schaffer M. Glioblastoma multiforme, diagnosis and treatment; recent literature review. Curr Med Chem 2017;24:3002–9.
2. Tan AC, Ashley DM, Lopez GY, Malinzak M, Friedman HS, Khasraw M. Management of glioblastoma: state of the art and future directions. CA Cancer J Clin 2020;70:299–312.

3. Cabrini G, Fabbri E, Lo Nigro C, Dechecchi MC, Gambari R. Regulation of expression of O6-methylguanine-DNA methyltransferase and the treatment of glioblastoma (Review). Int J Oncol 2015;47:417–28.
4. Hegi ME, Genbrugge E, Gorlia T, Stupp R, Gilbert MR, Chinot OL, et al. MGMT promoter methylation cutoff with safety margin for selecting glioblastoma patients into trials omitting temozolomide: a pooled analysis of four clinical trials. Clin Cancer Res 2019;25:1809–16.
5. Felsberg J, Thon N, Eigenbrod S, Hentschel B, Sabel MC, Westphal M, et al. Promoter methylation and expression of MGMT and the DNA mismatch repair genes MLH1, MSH2, MSH6 and PMS2 in paired primary and recurrent glioblastomas. Int J Cancer 2011;129:659–70.
6. Oldrini B, Vaquero-Siguero N, Mu Q, Kroon P, Zhang Y, Galan-Ganga M, et al. MGMT genomic rearrangements contribute to chemotherapy resistance in gliomas. Nat Commun 2020;11:3883.
7. Wang J, Cazzato E, Ladewig E, Frattini V, Rosenbloom DI, Zairis S, et al. Clonal evolution of glioblastoma under therapy. Nat Genet 2016;48:768–76.
8. Yu X, Erzinger MM, Pietsch KE, Cervoni-Curet FN, Whang J, Niederhuber J, et al. Up-regulation of human prostaglandin reductase 1 improves the efficacy of hydroxymethylacylfulvene, an antitumor chemotherapeutic agent. J Pharmacol Exp Ther 2012;343:426–33.
9. Gong J, Vaidyanathan VG, Yu X, Kensler TW, Peterson LA, Sturla SJ. Depurinating acylfulvene-DNA adducts: characterizing cellular chemical reactions of a selective antitumor agent. J Am Chem Soc 2007;129:2101–11.
10. Tanasova M, Sturla SJ. Chemistry and biology of acylfulvenes: sesquiterpene-derived antitumor agents. Chem Rev 2012;112:3578–610.
11. van Midwoud PM, Sturla SJ. Improved efficacy of acylfulvene in colon cancer cells when combined with a nuclear excision repair inhibitor. Chem Res Toxicol 2013;26:1674–82.
12. Koeppel F, Poindessous V, Lazar V, Raymond E, Sarasin A, Larsen AK. Irofulven cytotoxicity depends on transcription-coupled nucleotide excision repair and is correlated with XPG expression in solid tumor cells. Clin Cancer Res 2004;10:5604–13.
13. Wang J, Wiltshire T, Wang Y, Mikell C, Burks J, Cunningham C, et al. ATM-dependent CHK2 activation induced by anticancer agent, irofulven. J Biol Chem 2004;279:39584–92.
14. Wang Y, Wiltshire T, Senft J, Wenger SL, Reed E, Wang W. Fanconi anemia D2 protein confers chemoresistance in response to the anticancer agent, irofulven. Mol Cancer Ther 2006;5:3153–61.
15. Kathad U, Kulkarni A, McDermott JR, Wegner J, Carr P, Biyani N, et al. A machine learning-based gene signature of response to the novel alkylating agent LP-184 distinguishes its potential tumor indications. BMC Bioinf 2021;22:102.
16. Galli R, Binda E, Orfanelli U, Cipelletti B, Gritti A, De Vitis S, et al. Isolation and characterization of tumorigenic, stem-like neural precursors from human glioblastoma. Cancer Res 2004;64:7011–21.
17. Mao P, Joshi K, Li J, Kim SH, Li P, Santana-Santos L, et al. Mesenchymal glioma stem cells are maintained by activated glycolytic metabolism involving aldehyde dehydrogenase 1A3. Proc Natl Acad Sci U S A 2013;110:8644–9.
18. Guo G, Gong K, Puliyappadamba VT, Panchani N, Pan E, Mukherjee B, et al. Efficacy of EGFR plus TNF inhibition in a preclinical model of temozolomide-resistant glioblastoma. Neuro Oncol 2019;21:1529–39.
19. Lee EJ, Rath P, Liu J, Ryu D, Pei L, Noonepalle SK, et al. Identification of global DNA methylation signatures in glioblastoma-derived cancer stem cells. J Genet Genomics 2015;42:355–71.
20. Lopez-Bertoni H, Johnson A, Rui Y, Lal B, Sall S, Malloy M, et al. Sox2 induces glioblastoma cell stemness and tumor propagation by repressing TET2 and deregulating 5hmC and 5mC DNA modifications. Signal Transduct Target Ther 2022;7:37.
21. Viel T, Monfared P, Schelhaas S, Fricke IB, Kuhlmann MT, Fraefel C, et al. Optimizing glioblastoma temozolomide chemotherapy employing lentiviral-based anti-MGMT shRNA technology. Mol Ther 2013;21:570–9.
22. Yang H, Lou C, Sun L, Li J, Cai Y, Wang Z, et al. admetSAR 2.0: web-service for prediction and optimization of chemical ADMET properties. Bioinformatics 2019;35:1067–9.
23. Yoshino A, Ogino A, Yachi K, Ohta T, Fukushima T, Watanabe T, et al. Gene expression profiling predicts response to temozolomide in malignant gliomas. Int J Oncol 2010;36:1367–77.
24. Lee JC, Vivanco I, Beroukhim R, Huang JH, Feng WL, DeBiasi RM, et al. Epidermal growth factor receptor activation in glioblastoma through novel missense mutations in the extracellular domain. PLoS Med 2006;3:e485.
25. Talasila KM, Soentgerath A, Euskirchen P, Rosland GV, Wang J, Huszthy PC, et al. EGFR wild-type amplification and activation promote invasion and development of glioblastoma independent of angiogenesis. Acta Neuropathol 2013;125:683–98.
26. Tu Y, Xie P, Du X, Fan L, Bao Z, Sun G, et al. S100A11 functions as novel oncogene in glioblastoma via S100A11/ANXA2/NF-kappaB positive feedback loop. J Cell Mol Med 2019;23:6907–18.
27. Zhang B, Li H, Yin C, Sun X, Zheng S, Zhang C, et al. Dock1 promotes the mesenchymal transition of glioma and is modulated by MiR-31. Neuropathol Appl Neurobiol 2017;43:419–32.
28. Weeda G, van Ham RC, Masurel R, Westerveld A, Odijk H, de Wit J, et al. Molecular cloning and biological characterization of the human excision repair gene ERCC-3. Mol Cell Biol 1990;10:2570–81.
29. Alekseev S, Ayadi M, Brino L, Egly JM, Larsen AK, Coin F. A small molecule screen identifies an inhibitor of DNA repair inducing the degradation of TFIIH and the chemosensitization of tumor cells to platinum. Chem Biol 2014;21:398–407.
30. Borcsok J, Sztupinszki Z, Bekele R, Gao SP, Diossy M, Samant AS, et al. Identification of a synthetic lethal relationship between nucleotide excision repair deficiency and irofulven sensitivity in urothelial cancer. Clin Cancer Res 2021;27:2011–22.
31. Gabbard RD, Hoopes RR, Kemp MG. Spironolactone and XPB: an old drug with a new molecular target. Biomolecules 2020;10:756.
32. Stupp R, Mason WP, van den Bent MJ, Weller M, Fisher B, Taphoorn MJ, et al. Radiotherapy plus concomitant and adjuvant temozolomide for glioblastoma. N Engl J Med 2005;352:987–96.
33. Lin K, Gueble SE, Sundaram RK, Huseman ED, Bindra RS, Herzon SB. Mechanism-based design of agents that selectively target drug-resistant glioma. Science 2022;377:502–11.
34. Eckhardt S, Csetenyi J, Horvath IP, Kerpel-Fronius S, Szamel I, Institoris L, et al. Uptake of labeled dianhydrogalactitol into human gliomas and nervous tissue. Cancer Treat Rep 1977;61:841–7.
35. Peng C, Qi XM, Miao LL, Ren J. 1,2:5,6-dianhydrogalactitol inhibits human glioma cell growth *in vivo* and *in vitro* by arresting the cell cycle at G_2–M phase. Acta Pharmacol Sin 2017;38:561–70.
36. Hu K, Fotovati A, Chen J, Triscott J, Bacha J, Brown D, et al. Abstract 811: VAL083, a novel N7 alkylating agent, surpasses temozolomide activity and inhibits cancer stem cells providing a new potential treatment option for glioblastoma multiforme. In: Proceedings of the 103rd Annual Meeting of the American Association for Cancer Research; 2012 Mar 31–Apr 4; Chicago, IL. Philadelphia (PA): AACR; Abstract nr 811.
37. Chauhan AK, Li P, Sun Y, Wani G, Zhu Q, Wani AA. Spironolactone-induced XPB degradation requires TFIIH integrity and ubiquitin-selective segregase VCP/p97. Cell Cycle 2021;20:81–95.
38. Wedge SR, Newlands ES. O6-benzylguanine enhances the sensitivity of a glioma xenograft with low O6-alkylguanine-DNA alkyltransferase activity to temozolomide and BCNU. Br J Cancer 1996;73:1049–52.
39. Chawla S, Rockstroh A, Lehman M, Ratther E, Jain A, Anand A, et al. Gene expression based inference of cancer drug sensitivity. Nat Commun 2022;13:5680.
40. Dorman SN, Baranova K, Knoll JH, Urquhart BL, Mariani G, Carcangiu ML, et al. Genomic signatures for paclitaxel and gemcitabine resistance in breast cancer derived by machine learning. Mol Oncol 2016;10:85–100.
41. Reinhold WC, Sunshine M, Varma S, Doroshow JH, Pommier Y. Using cellminer 1.6 for systems pharmacology and genomic analysis of the NCI-60. Clin Cancer Res 2015;21:3841–52.
42. Cancer Genome Atlas Research Network. Comprehensive genomic characterization defines human glioblastoma genes and core pathways. Nature 2008;455:1061–8.
43. Leung WH, Vong QP, Lin W, Janke L, Chen T, Leung W. Modulation of NKG2D ligand expression and metastasis in tumors by spironolactone via RXRgamma activation. J Exp Med 2013;210:2675–92.
44. Xavier MA, Rezende F, Titze-de-Almeida R, Cornelissen B. BRCAness as a biomarker of susceptibility to PARP inhibitors in glioblastoma multiforme. Biomolecules 2021;11:1188.
45. Cerami E, Gao J, Dogrusoz U, Gross BE, Sumer SO, Aksoy BA, et al. The cBio cancer genomics portal: an open platform for exploring multidimensional cancer genomics data. Cancer Discov 2012;2:401–4.
46. Sulkowski PL, Corso CD, Robinson ND, Scanlon SE, Purshouse KR, Bai H, et al. 2-Hydroxyglutarate produced by neomorphic IDH mutations suppresses homologous recombination and induces PARP inhibitor sensitivity. Sci Transl Med 2017;9:eaal2463.